Journal of Extracellular Vesicles

RESEARCH ARTICLE OPEN ACCESS

RNAs Associated With Bacterial Outer Membrane Vesicles: Structural Insights Into Surface Composition

Kevin Mosca[1,2,3] | Florian Turbant[1,2] | Wafa Achouak[4] | Frank Wien[2] | Véronique Arluison[1,2,5]

[1]Laboratoire Léon Brillouin, UMR 12 CEA/CNRS, CEA Saclay, Gif-sur-Yvette, France | [2]L'Orme des Merisiers Saint Aubin, Synchrotron SOLEIL, Gif-sur-Yvette, France | [3]Biochemistry and biophysics mRNA unit, mRNA Center of Excellence, Analytical Sciences, Sanofi, Marcy l'Etoile, France | [4]Lab of Microbial Ecology of the Rhizosphere, (LEMiRE), BIAM, Aix Marseille University, CEA, CNRS, Saint Paul Lez Durance, France | [5]UFR Sciences du Vivant, Université Paris Cité, Paris, France

Correspondence: Véronique Arluison (veronique.arluison@u-paris.fr)

Received: 8 December 2025 | **Revised:** 13 March 2026 | **Accepted:** 8 May 2026

Keywords: Bacterial amyloid | Hfq | Host immune response | Membrane insertion | Outer Membrane Vesicle (OMV) | RNA | Synchrotron Radiation Oriented Circular Dichroism SR-O-CD | Trans-kingdom communication

ABSTRACT

Gram-negative bacteria release outer membrane vesicles (OMVs) that deliver various molecules, including virulence factors, allowing them to interact with their host. Recent evidence suggests that OMVs may serve as carriers for RNAs, in particular small regulatory noncoding RNAs (sRNAs). However, for these sRNAs to function effectively, they often require a protein cofactor, typically the Hfq RNA chaperone. In our previous studies, we demonstrated that Hfq, after interacting with the bacterial inner membrane, can be translocated to the periplasm and subsequently exported within OMVs, potentially in association with RNAs. In the present study, we build upon this previous work and provide evidence that RNA molecules are not only a key component of the OMV lumen, but can also be inserted into the vesicle membrane in an Hfq-dependent manner. This new finding suggests that surface-presented RNAs may be directly delivered to the host. Overall, our results reveal a previously unrecognized aspect of OMV-associated RNA and emphasizes the need to explore the role of RNAs in cell-to-cell communication, as OMV-host interplay may not be governed solely by protein-protein or protein-membrane contacts.

1 | Introduction

Bacteria are remarkably adaptable organisms capable of adjusting their gene expression to thrive in diverse environments. This adaptability is primarily achieved *via* regulatory networks that control gene expression in response to external signals, as well as by interbacterial communication. A key component of this communication involves outer membrane vesicles (OMVs) (Sartorio et al. 2021). OMVs are nanosized spherical structures (~100 nm in diameter) released by Gram-negative bacteria through blebbing of the outer membrane (Furuyama and Sircili 2021; Kulp and Kuehn 2010). They play critical roles in cell-to-cell and trans-kingdom communication, stress responses during host infection, virulence, increased antibiotic resistance, as well as in host immunomodulation (Blenkiron et al. 2016; Lee 2019; Sartorio et al. 2021; Schwechheimer and Kuehn 2015; Tsatsaronis et al. 2018; Zhang et al. 2025). Originating from the bacterial outer membrane (OM), the composition of OMVs reflects that of the OM, primarily comprising phospholipids, lipopolysaccharides (LPS), and outer membrane proteins. Internally, OMVs also contain components referred to as cargo, which include proteins, amino acid residues, sugars, peptidoglycan fragments or toxins

Kevin Mosca and Florian Turbant are Joint First Authors.

(Dauros-Singorenko et al. 2018; Furuyama and Sircili 2021). OMVs deliver diverse biomolecules to host cells or neighbouring bacteria (Schwechheimer and Kuehn 2015; Tsatsaronis et al. 2018). Beyond proteins, OMVs carry RNAs, including regulatory noncoding RNAs, tRNAs, rRNAs, and mRNAs, recognized as novel virulence factors, though the roles of larger transcripts remain less explored (Blenkiron et al. 2016; Ghosal et al. 2015; Koeppen et al. 2016; Malabirade et al., 2018). Both full-length RNAs and fragments are present in OMVs (Diallo et al. 2022b). Although mechanisms are not fully understood, bacterial vesicular RNAs can alter host gene expression and modulate immune responses. For instance, RNAs from uropathogenic *Escherichia coli* OMVs are delivered to host cells (Blenkiron et al. 2016); sRNAs from *E. coli* regulate gene expression and physiology in *Caenorhabditis elegans* (Liu et al. 2012); and *Pseudomonas aeruginosa* vesicular sRNAs suppress host MAP kinase expression and reduce LPS-induced cytokine production (Koeppen et al. 2016). Additionally, tRNA-derived fragments may post-transcriptionally regulate host genes in an Argonaute-dependent manner (Diallo et al. 2022b; Kuscu et al. 2018). OMVs also contain pathogen-associated molecular patterns (PAMPs), such as LPS and lipoproteins, which activate pattern recognition receptors (PRRs), including TLRs (Pandey et al. 2014). Bacterial LPS triggers TLR4-mediated pro-inflammatory cytokine production, while RNAs may be recognized by TLR7, TLR8, or TLR13, activating inflammatory pathways (Mancini et al. 2020). Through membrane association and internalization, OMV cargo can deliver signalling molecules that modulate host cell functions, promote bacterial survival, and influence immune responses. In particular, OMV RNAs may help pathogens evade immune detection or alter host signalling via cytokine induction (Ha et al. 2020).

Among key factor that enable bacteria to respond to external signals are small regulatory noncoding RNAs, sRNAs (Papenfort and Melamed 2023). Typically, 100–200 nucleotides in length, these sRNAs regulate gene expression at the post-transcriptional level by imperfectly base-pairing with their mRNAs target, thereby influencing mRNA stability and translation (Gottesman 2019; Kavita et al. 2018; Vigoda et al. 2024). sRNAs are found in almost all prokaryotes (Gelsinger and DiRuggiero 2018), and extensive studies, in particular in Gram negative bacteria, have revealed their critical roles in diverse biological functions, including virulence or nutriment acquisition (Pulvermacher et al. 2009; Rice and Vanderpool 2011; Svensson and Sharma 2016). For instance, in the context of iron homeostasis, several sRNAs have been identified as key regulators of iron uptake and recycling, enabling bacteria to survive within the host environment where iron availability is limited (Salvail and Masse 2012). The mechanism of sRNAs-mediated regulation typically involves base-pairing with specific regions in the 5' untranslated region (5′ UTR) of their target mRNA, particularly around the translation initiation region, which includes the ribosome binding site (RBS) and the start codon AUG. This interaction can either prevent or promote the binding of the 30S ribosomal small subunit, thereby modulating translation initiation (Gottesman 2019; Majdalani et al. 1998). sRNA-mediated regulation often involves additional protein factors, such as Hfq or ProQ, which act as RNA chaperones to facilitate sRNA-mRNA interactions (Melamed et al. 2020). However, the mechanisms of action of these two proteins are distinct. Hfq, for instance, not only facilitates sRNA:mRNA pairing but can also mediate mRNA degradation independently of sRNAs. In Gram negative bacteria, polyadenylation, the post-transcriptional addition of a stretch of adenine residues by poly(A) polymerase (PAP), typically marks RNA for degradation by exonucleases (De Lay et al. 2013; Hajnsdorf et al. 1995). As an RNA chaperone, Hfq increases the PAP efficiency, leading to a subsequent RNA degradation. (Hajnsdorf and Régnier 2000). Among the Hfq-dependent polyadenylated RNAs targeted for degradation is the *rpsO* mRNA, which encodes the ribosomal protein S15 (Haugel-Nielsen et al. 1996). Notably, polyadenylated *rpsO* mRNA, exhibits one of the highest known affinities for Hfq with a dissociation constant (K_d) in the tens of picomolar range (Folichon et al. 2003). Thus, Hfq contribute to mRNAs destabilization through both sRNA-dependent and polyadenylation-dependent pathways. Importantly, sRNAs in *E. coli* can be polyadenylated, and this modification predominantly facilitates their degradation, as it does for mRNAs (Maes et al. 2017). Conversely, Hfq may also protect sRNAs from ribonucleic degradation (Folichon et al. 2003; Moll et al. 2003).

Structurally, the N-terminal region (NTR) of *E. coli* Hfq assembles into a torus-shaped hexamer, with six C-terminal regions (CTR, 38 amino acid residues) extending outward from the core structure (Arluison et al. 2004; Brennan and Link 2007). The hexameric assembly and RNA annealing function of Hfq primarily arises from its NTR (Vogel and Luisi 2011). Until recently, the role and structure of the elongated CTR remained poorly understood; however, recent studies, have shown that it can adopt an amyloid-like conformation (Berbon et al. 2023; Fortas et al. 2015). The role of the CTR in RNA annealing remains debatable: it appears largely dispensable for most sRNA-mediated regulation (Olsen et al. 2010), although its absence may impact some specific sRNA-based regulatory events (Salim et al. 2012; Turbant et al. 2021; Vecerek et al. 2008; Vincent et al. 2012). An important aspect of Hfq-CTR function lies in its interaction with the bacterial membrane (Malabirade et al. 2017; Turbant et al. 2022). This interaction was initially observed *in vivo* using imaging techniques (Diestra et al. 2009; Taghbalout et al. 2014), although at the time, direct interaction-binding remained unclear. It was estimated that around 50% of Hfq localizes near the inner membrane (Diestra et al. 2009). Several hypotheses have been proposed to explain this interaction, including binding to a membrane-associated RNase or a post-translational modification such as an oxidized C18 lipid (Ikeda et al. 2011; Obregon et al. 2015; Taghbalout et al. 2014). However, recent evidence demonstrates that, the C-terminal region of Hfq can directly engage the inner membrane without requiring intermediary proteins or post-translational modifications, leveraging the intrinsic ability of amyloid-like structure to interact with lipid bilayers (Qiang et al. 2015). Molecular microscopy studies further revealed that Hfq-membrane interactions can induce membrane deformation and rupture (Malabirade et al. 2017; Turbant et al. 2022). Notably, Hfq associates with both the inner and outer membranes (IM/OM) of Gram-negative bacteria (Turbant et al. 2023; Turbant et al. 2022), raising the possibility that Hfq may reside in the periplasm space, and subsequently be encapsulated within OMV as cargo (Turbant et al. 2023). Transmission electron microscopy (TEM) localization has suggested that Hfq is present in the periplasmic space (Diestra et al. 2009). However, the limits of TEM's resolution prevent a definitive localization of Hfq between the inner and outer membranes.

Hfq may thus play a crucial role in selectively packaging RNA cargo into OMVs through the coordinated actions of its structural domains. The CTR of Hfq is essential for membrane poration, enabling both the protein and its RNA cargo to cross the inner membrane into the periplasm. Once in the periplasm, the N-terminal region of Hfq binds to and stabilizes specific RNAs, protecting them and promoting their incorporation into OMVs. This process likely involves direct interactions between Hfq and the vesicle formation machinery to ensure efficient RNA packaging during OMV biogenesis. Consistent with this model, Hfq has been found in *E. coli* and *Proteus mirabilis* OMVs. (Gonzalez et al. 2024; Turbant et al. 2023). Moreover, Hfq's role in stress response may influence the selection of RNA cargo, thereby modulating the role of OMVs in intercellular communication, immune response, and environmental adaptation.

In the present study, we build upon our previous work by demonstrating that *E. coli* Hfq, using its CTR, interacts with the outer membrane (Turbant et al. 2023). Specifically, we show that Hfq facilitates the insertion of RNAs into the membrane of OMVs, derived from the Gram*(-)* OM. This interaction between RNA and the OM may play a crucial role in RNA-mediated regulatory processes (Eason et al. 2019; Frohlich and Gottesman 2018; Kannaiah et al. 2019). RNAs associated with OMVs could for instance regulate gene expression in recipient cells (Ajam-Hosseini et al. 2023), providing a mechanism by which bacteria influence host gene expression and immune cell differentiation. As surface-exposed RNAs can be recognized by host recognition receptors (such as Toll-like receptors), they could potentially trigger or regulate innate immune response (Shimizu 2024). Thus, OMV-associated RNAs represent a promising target for the development of novel therapeutic strategies against bacterial infections (Ajam-Hosseini et al. 2023).

Synchrotron Radiation Oriented Circular Dichroism (SR-O-CD), an absorption spectroscopy derived from Circular Dichroism (CD), measures how chiral molecules in a sample interact with polarized light. CD measures the difference in absorption of left- and right-circularly polarized light by chromophores in a chiral environment. It is widely used to study the structure of biological macromolecules in solution, where the molecules are randomly oriented; consequently, the measured signal reflects the average across all molecular orientations (i.e., the system is isotropic). Compared to conventional CD, Synchrotron Radiation Circular Dichroism (SRCD) offers an extended wavelength range down to the vacuum ultraviolet (VUV), thereby increasing the spectral information content and improving structural insights (Miles and Wallace 2006; Mosca et al. 2026). This extension is limited to 168 nm for hydrated samples due to strong water absorption in the far-UV. The SR-O-CD technique is a variant of circular dichroism spectroscopy based on the phase modulation of linearly polarized light at a quarter wavelength ($\lambda/4$). When a sample contains UV-transparent membranes with chiral chromophores (such as proteins), these chromophores can align within the membrane and become anisotropic. This alignment creates linear dichroism (LD) in addition to the usual circular dichroism (CD) signal (Hoffmann et al. 2026). Dependent on the orientation of the inserted or membrane-embedded chromophores, the circular dichroism absorption measurement will be impacted by this additional linear absorption. When the sample is rotated along the centred incident beam, the angle between incident beam and the oriented chromophores induces a linear absorption variation that depends on the rotation angle. This linear dichroism (LD) contribution impacts the CD absorption but also allows identification of the oriented chromophores. Rotating the sample around the beam changes the angle and therefore the LD contribution. Using this property, LD absorption can be cancelled out by rotating the sample through 360° and recording spectra at different angles (e.g., every 45°). Averaging these spectra cancels out LD contributions, leaving the oriented circular dichroism (OCD) signal (Bürck et al. 2016; Wu et al. 1990).

2 | Materials and Methods

2.1 | Preparation of the C-terminal Region of Hfq and rpsO RNAs

The Hfq-CTR peptide (residues 64 to 102 of full-length Hfq), and the *rspO* RNA sequences were chemically synthetized (Proteogenix/France and Eurogentec/Belgium, respectively). The sequence SRPVSHHSNNAGGGTSSNYHHGSSAQNTSAQ QDSEETE of the CTR peptide was prepared at 20 mg/mL, following the procedure outlined by Fortas et al. (Fortas et al. 2015). The *rspO* RNA sequence (corresponding to the end of full *rpsO* mRNA) used here was the following (Folichon et al. 2003):

rspO: CAGAAAAGGGGGCCUGAGUGGCCCCUUUUUUC

The sequence of polyadenylated *rpsO* mRNA (referred as *rpsO-polyA*) was:

rspO-polyA: CAGAAAAGGGGGCCUGAGUGGCCCCUUUUU-UCAAAAAAAAAAAAAAAAAA

Finally, as a control we also used a polyA sequence, corresponding to the same polyA tail than that of *rspO-polyA*, but devoid of the *rpsO* part

polyA: AAAAAAAAAAAAAAAAAA

The RNAs were prepared in sterile Molecular Biology grade water at 1 mM (concentration expressed in in strand)

2.2 | Preparation of Outer Membrane Vesicles (OMVs)

The *E. coli* MG1655 Δ*hfq* strain was grown in LB for 24 h at 37°C with shaking (140 rpm). The Δ*hfq* mutant was used to avoid Hfq contamination in OMV membranes for SR-O-CD experiments. Cultures (300 mL) were centrifuged twice at 8,000 × g for 30 min, and the supernatant was filtered (0.22 µm PES). OMVs were collected by ultracentrifugation at 150,000 × g, 4°C for 2 h and resuspended in sterile PBS. To remove RNAs associated with the OMV surface, samples were treated with RNase A/T1 (37°C, 1 h), followed by enzyme removal using a 30 kDa Amicon centrifugal filter. OMVs were subsequently purified by density gradient ultracentrifugation using OptiPrep (60% iodixanol; Sigma-Aldrich). Gradients were prepared in sterile PBS with six layers (45%, 40%, 35%, 30%, 25%, and 20%) and centrifuged at 150,000 × g at 4°C for 20 h. OMV-containing fractions were identified by light scattering

analysis (Zetasizer, Malvern) and by fluorescence labelling with the lipophilic dye FM1-43 (5 μg/mL). Fractions enriched in OMVs were pelleted by ultracentrifugation at 200,000 × g for 2 h at 4°C to remove OptiPrep, resuspended in sterile PBS, and stored at −80°C until SR-O-CD analysis. The concentration of OMVs was measured using a Nanoparticle Tracker Analyzer (NTA) (Blache and Achouak 2024). The protein concentration of the samples was measured using a Bradford assay (Bradford 1976) and confirmed by OD measurement at 280 nm. OMV purity, size, and integrity were assessed using Transmission Electron Microscopy (TEM) with negative staining using 0.1% phosphotungstic acid. TEM analysis indicated the absence of significant amounts of flagella, fimbriae and pili in preparations from the Δ*hfq* strain compared to WT. OMVs were however subjected to density gradient to remove the residual flagella or pili (Welsh et al. 2024).

2.3 | Preparation of OM-Supported Membranes for Synchrotron Radiation Oriented Circular Dichroism SR-O-CD Analysis

For the formation of supported membranes (OCD requires the membrane to be immobilized on a flat solid surface), $CaCl_2$ was added to the OMV solution to a final concentration of 3 mM. A 20 μL aliquot of the mixture was placed on a CaF_2 surface cell and incubated for 1 hour at room temperature (RT). Excess of OMVs were rinsed five times with deionized water to remove any unbound membranes. The supported OM was kept wet in a chamber containing a saturated K_2SO_4 solution, ensuring 97% humidity at 26°C.

2.4 | Synchrotron Radiation Circular Dichroism (SRCD) and Synchrotron Radiation Oriented Circular Dichroism SR-O-CD

SRCD analysis measurements were conducted on the DISCO beamline at Synchrotron SOLEIL (proposal 20231277). SRCD offers higher signal intensity and access to shorter wavelengths than conventional CD, allowing more sensitive and detailed analysis of RNA secondary structure (Mosca et al. 2026). A sample volume of 4 μL was placed into circular demountable CaF_2 cells with a 20 μm pathlength (Wien and Wallace 2005). Spectral data were recorded in triplicates over the wavelength range from 320 nm to 180 nm, with 1 nm intervals and a 1.2-second integration time at 20°C for both the sample and baseline measurements. (+)-camphor-10-sulfonic acid (CSA) was used for calibration. Data processing, which included averaging, baseline subtraction, smoothing and scaling was carried out using CDtoolX (Miles and Wallace 2018). The concentrations of the individual RNAs and proteins as well as for the complex were maintained using the same cell and pathlength to enable the comparison of spectra with each other. For melting curve acquisitions, the scans were conducted from 10°C to 95°C in 3°C increments. Melting curves were fitted using a Gibs-Helmholtz equation: (Shih et al. 1995)

For SR-O-CD measurements, OMVs were first deposited on the surface of the CaF_2 cell (20 μm pathlength) following the protocol described by Turbant et al. (Turbant et al., 2024a). Thin lipid films were employed to minimize scattering and to ensure sample homogeneity (see also below). A CaF_2 lid was placed over the sample to maintain humidity inside the closed cell, ensuring airtight conditions. The CTR and/or RNA solutions were applied on top of the OMV film. A washing procedure was performed after each step of insertion to remove any excess CTR and/or RNA (Turbant et al., 2024a). It should be noted that the kinetics of insertion typically takes several hours, and SR-O-CD spectra were recorded continuously throughout this process by rotating the sample in 45° increments using an automated rotating chamber (Wien et al. 2013). The rotation effectively eliminated linear dichroism caused by the orientation of peptide/RNA on or within the membrane. The resulting SR-O-CD spectra, average of the rotation-spectra, were analysed as described by Turbant et al. (Turbant et al., 2024a). The reduction in circularly polarized light absorption, resulting from changes in the transition dipoles (n-π^* and π-π^* transitions for the protein π-π^* for the RNA), is responsible for the observed variation in SR-O-CD signal amplitude. Briefly, if the protein/RNA orientation shifts from lying parallel to the membrane to being inserted into the membrane, the SR-O-CD signal should decrease significantly (Bürck et al. 2016; Turbant et al., 2024b; Waeytens et al. 2022). The uniformity of the thin film was verified by light microscopy and by following the High Tension (HT) profile through-out the spectral range assuring homogenity between recordings of the resulting absorbances at each angle. The HT variation was in the 1%–2% range and thus negligible.

3 | Results

In this study, we expand on our previous findings about consequences of Hfq insertion within the OM (Turbant et al., 2024a). While the association of Hfq and RNA with OMVs have been established previously (Ghosal et al. 2015; Turbant et al. 2023), Hfq may be exported in OMVs alongside RNAs. Here, we intend to show that RNA molecules can not only be internalized in the OMV lumen, but that they can also integrate into the vesicle membrane in an Hfq-dependent manner. To explore this novel characteristic of OMV, we introduced a novel application of synchrotron-based circular dichroism (SRCD). Specifically, to decipher the role of Hfq in RNA insertion into the OMV membrane, we employed the innovative technique of Synchrotron Radiation Oriented Circular Dichroism (SR-O-CD) spectroscopy, applied here for the first time to this system (Bürck et al. 2016; Waeytens et al. 2022). Indeed, the heterogeneous nature of the OMV surface makes the analysis of RNA insertion particularly challenging. We previously demonstrated that Hfq and its CTR can be inserted inside OMV membranes (Turbant et al. 2023). Here, we applied the same experimental approach to analyse the insertion of a part of mRNA, namely the *rpsO-polyA* RNA. We selected this particular mRNA because it exhibits the highest affinity for Hfq among all tested nucleic acids. Indeed, the polyadenylated *rpsO* mRNA:Hfq complex exhibits an equilibrium dissociation constant K_D about tens of pM (Folichon et al. 2003). Since sRNAs *in E. coli* are also subject to polyadenylation, *rpsO-polyA* provides a model for studying polyadenylated transcripts in general (Maes et al. 2017).

For our SR-O-CD experiments, we used OMVs derived from a Δ*hfq* mutant strain to prevent prior inclusion of Hfq in the OMV membranes. The concentration of OMVs measured using a Nanoparticle Tracker Analyzer was $1.95 \pm 0.45 \times 10^{10}$

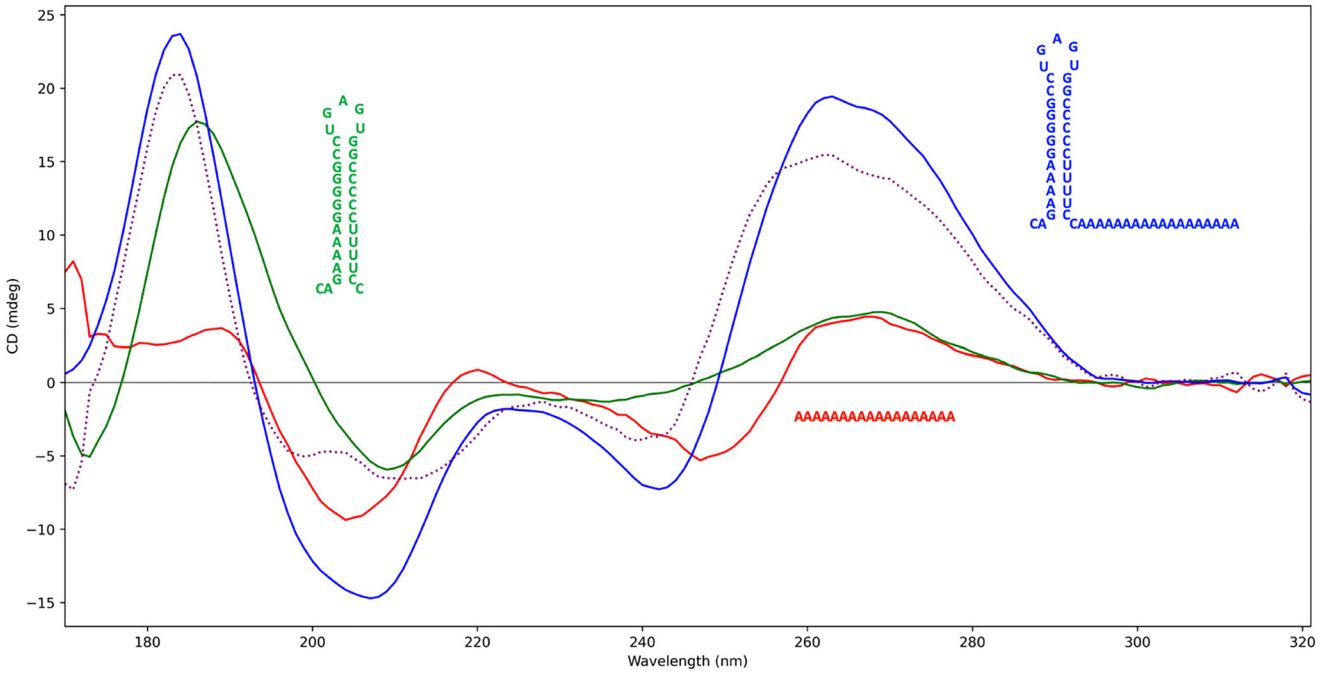

FIGURE 1 | **Synchrotron Radiation Circular Dichroism (SRCD) spectra of *rpsO-polyA*, *rpsO* and *polyA RNA***. Blue: *rpsO-polyA*; Green: *rpsO*; Red: *polyA* (18 nucleotides); Dotted purple line: theoritical spectrum of *rpsO-polyA* minus polyA. The *rpsO-polyA* spectrum exhibits two maxima at 263 nm and 183 nm, and two minima at 207 nm and 242 nm, which correspond to the minimum observed in the polyA spectrum at 247 and 204 nm. In contrast, the *rpsO* spectrum shows two maxima at 269 nm and 186 nm, and one minimum at 215 nm. Note that the spectral range is limited below ~170 nm due to strong water absorption in the far-UV.

particles/mL. Notably, the OMV yield per bacterial cell from the Δ*hfq* strain was at least 10-fold higher than that from the WT strain, likely due to Hfq-dependent regulation of the PhoP/PhoQ system, which directly influences OMV biogenesis (Bonnington and Kuehn 2017; Coornaert et al. 2010). The protein concentration of the samples was approximately 820 μg/mL and the RNA concentration was 52 μg/mL, corresponding to ~0.6 nmol of RNA (expressed in nucleotides) in the 4 μL SR-O-CD sample. The 260/280 ratio of 1.88 observed confirms that the OD signal predominantly arises from nucleic acids signal (most likely RNA), but that there is a mixture of RNA plus some proteins (Figure. S1). OMV purity, size, and integrity were assessed using Transmission Electron Microscopy (TEM). TEM analysis confirmed the absence of significant amounts of flagella, fimbriae and pili in preparations from the Δ*hfq* strain compared to WT strain, as expected (De Lay and Gottesman 2012) (Figure. S2). OMVs isolated from the Δ*hfq* strain ranged from 20 to 100 nm in diameter, slightly smaller than those obtained from WT cells, and showed no evidence of a substantial population of outer–inner membrane vesicles (OIMVs) (Figure. S2).

3.1 | Hfq-CTR Binds and Melts rpsO-polyA

First, we characterized *rpsO-polyA* RNA using conventional SRCD and compared its spectrum with those of *rpsO* and *polyA* RNAs (Figure 1). The spectrum of *rpsO* differs from the spectrum difference obtained by subtracting *polyA* from *rpsO-polyA*, suggesting that polyA addition changes the global folding of *rpsO* RNA.

We then evaluated the effect of Hfq and, more precisely, that of its CTR on *rpsO* RNA stability (Figure 2). The presence of the CTR did not significantly affect the stability of any of the RNA sequences, except for *rpsO-polyA* in the presence of Hfq-CTR, where the T_m was slightly reduced. This result, in agreement with previous reports, indicates that Hfq binding causes subtle conformational changes in the polyadenylated *rpsO* mRNA (Folichon et al. 2003).

3.2 | OMVs May Carry RNA Externally and Internally

Next, using SR-O-CD, we analysed the insertion of *rpsO-polyA* in OMV membrane using OMVs containing pre-inserted CTR peptides (Figure 3). Purified OMVs from an Hfq-deficient strain were supplemented with CTR peptides.

Here, the OMV membrane-associated peptide and/or RNA are oriented within the lipid membrane (they can be aligned parallel or perpendicular to the membrane plane), and the coupling between the transition dipole moments of the chromophores and the incident circularly polarized light becomes directionally dependent. When the sample cell containing the aligned bilayers is rotated by 180°, the orientation of the ordered system relative to the light propagation axis is reversed for specific regions of the spectrum. The OCD signal depends on the alignment of the chromophores' transition dipole moments with the light's electric field. The spatial arrangement and orientation of the chromophores therefore reverses the sign of the spectrum, which

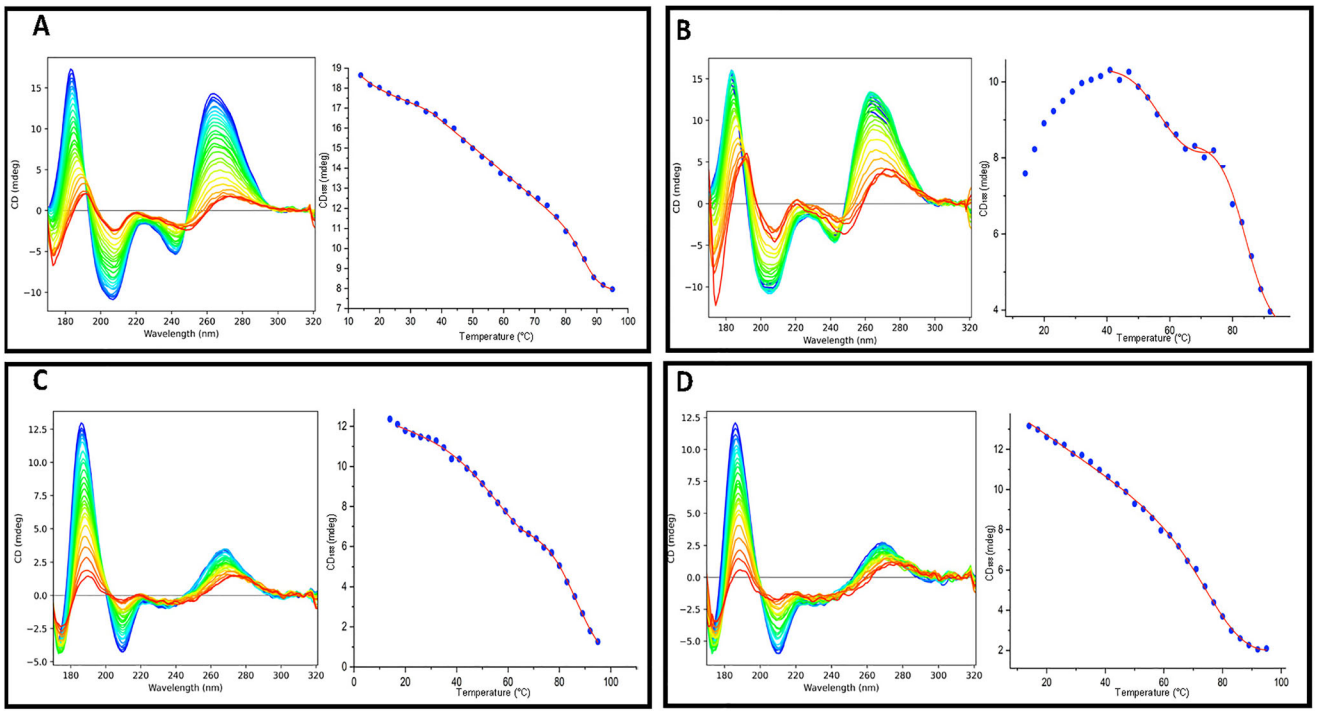

FIGURE 2 | Synchrotron Radiation Circular Dichroism (SRCD) thermal denaturation spectra of *rpsO* and rpsO-polyA, with and without CTR and their correspoding melting curves taken at 182 nm. Thermal scans were measured from 15 to 96°C, blue corresponding to lower temperatures and red to highest temperatures. A: *rpsO*-polyA. B: *rpsO*-polyA in presence of the CTR, C: *rpsO*. D: *rpsO* in presence of CTR. Note that the left parts of A and B are the same as in Figure 1, but are shown again for a better comparison between the spectra with CTR. The T_m measured at 182 nm were for *rpsO*-polyA (A): 86.8±2.5°C; *rpsO*-polyA+CTR (B): 58.2±0.8° and 84.1±0.7°C (note also the increased stability in the presence of the CTR at low temperature in this case); *rpsO* (C): 85±0.5°C; and *rpsO*+CTR (D): 82.6°±3.5C. The reduction in the amplitude of the 182 nm peak reflects helical backbone melting, but fitting the melting curves at 265 nm (which reflects base pairing and stacking) does not significantly differ from those at 185 nm. These T_m indicate that Hfq CTR does not influence significantly the RNAs stability, except for the polyA tailed *rpsO*, where Tm is partially reduced.

may partially invert depending on the rotation angle (i.e., positive bands become negative and *vice versa*).

The SR-O-CD spectrum of CTR pre-inserted into OMVs is presented in the inset of Figure 3. As shown in this inset, we observe a progressive decrease in OCD amplitudes during CTR interaction with the OMV membrane, indicating that the protein is being inserted into the OMV. We also confirm that the CTR inserted into the OMVs is structured in an amyloid-like conformation (indicated by the minimum observed around 220 nm (Waeytens et al. 2022)). Subsequently, *rpsO-polyA* RNA was added to OMVs containing pre-inserted Hfq-CTR. After incubation, the excess non-inserted CTR was washed away as described in the Methods section. The *rpsO-polyA* RNA was found to associate with the OMV membrane, leading to a change in the SR-O-CD spectra at specific rotational angles (figure 3). Specifically, insertion of the polyA-tailed *rpsO* into the OMVs was evidenced by the spectral inversion around 200 nm. This inversion is a characteristic feature of oriented samples and indicates that the measured signal arises from anisotropic molecular alignment. Together with the washing of OMVs to remove unbound RNA, this observation confirms that the RNA is bound and oriented within the OMV membrane. Importantly, this insertion depends on the presence of the Hfq-CTR, which itself integrates into the membrane, as in the absence of CTR, no RNA insertion was observed (Figure 4).

Next, we tested the possible interaction of non-polyadenylated *rpsO* RNA with the OMV membrane, both in the presence and absence of pre-inserted CTR peptides. Unlike *rpsO-polyA*, *rpsO* RNA did not exhibit spectral inversion, indicating the absence of significant RNA insertion into the OMVs (Figure 5). Nevertheless, rotation-dependent variation in signal intensity still indicates that RNA interacts with the OMVs.

Finally, we also tested the possible insertion of short polyA in the membrane. As shown in figure 6, a slight insertion of polyA (rA_{18}) occurs, indicated by the spectral change depending on the orientation. This insertion occurred only in the presence of pre-inserted CTR peptides in the OMVs, as shown in the inset of figure 6.

From these observations, we can thus conclude that: *(i) rpsO* binds to the OMV membrane *via* Hfq-CTR, and *(ii)* membrane insertion occurs primarily when the RNA is polyadenylated, probably due to the high affinity of the CTR for A-rich sequences (Folichon et al. 2003).

4 | Discussion

While the *in vivo* consequences of RNAs associated with OMVs were not directly investigated in the present study, our findings

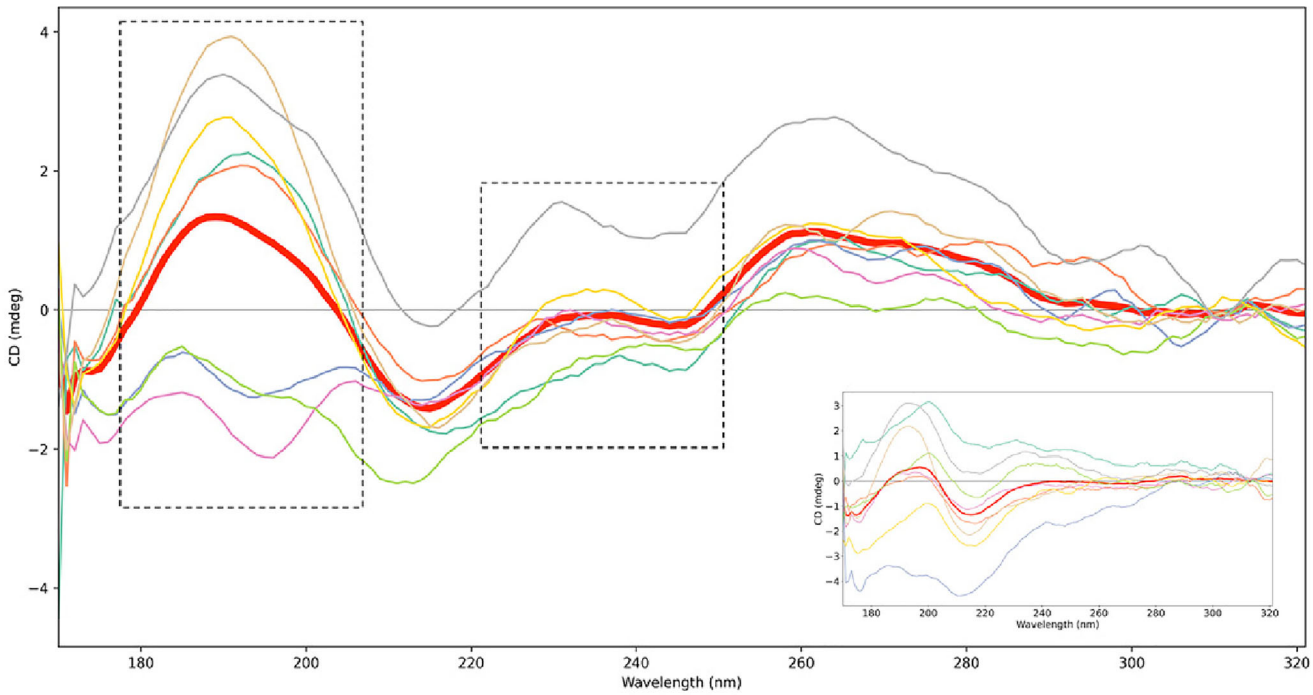

FIGURE 3 | **Oriented Synchrotron Radiation Circular Dichroism (SR-O-CD) analysis of the CTR-mediated insertion of *rpsO-polyA* RNA with OMV supported membrane**. Thin lines: Spectra at different rotation angles of the sample obtained after washing. Red bold line: Mean of the spectra at different orientations. The signal inversion (highlighted by black-dotted frames), characteristic of oriented samples, indicates anisotropic molecular alignment and, together with washing of OMVs to remove unbound *rpsO-polyA* RNA, confirms that RNA is bound and oriented within the OMV membrane. Note that CD units cannot be expressed in delta epsilon ($\Delta\varepsilon$) for a complex between two different molecules of different nature, such as a protein and RNA in this case. Inset: Control of CTR pre-insertion inside the OMV membrane. Notably, the same analysis with full protein is particularly difficult due to presence of the Sm ring in the NTR part, mainly composed of β-sheets but with a variable orientation throughout the torus. This makes it difficult to conclude with the full-length protein orientation (Turbant et al., 2024b).

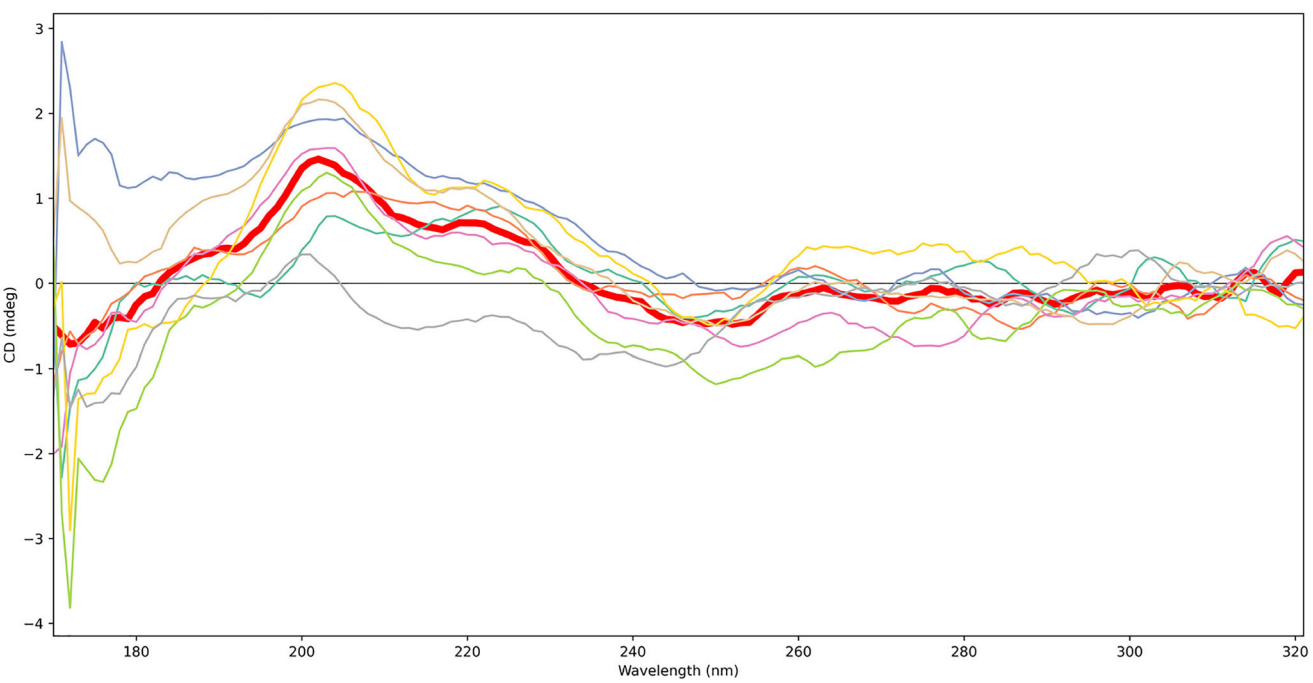

FIGURE 4 | **SR-O-CD analysis of the interaction of *rpsO-polyA* RNA with OMV supported membrane in the absence of Hfq**. Thin line: Spectra at different rotation angles obtained after washing. Red bold line: Mean of the spectra at different orientations. The weak variation of signal intensity and absence of characteristic nucleic acid spectral features e.g. 260–280 nm absorption indicates that the *rpsO-polyA* mRNA does not insert into the OMVs and has been washed away.

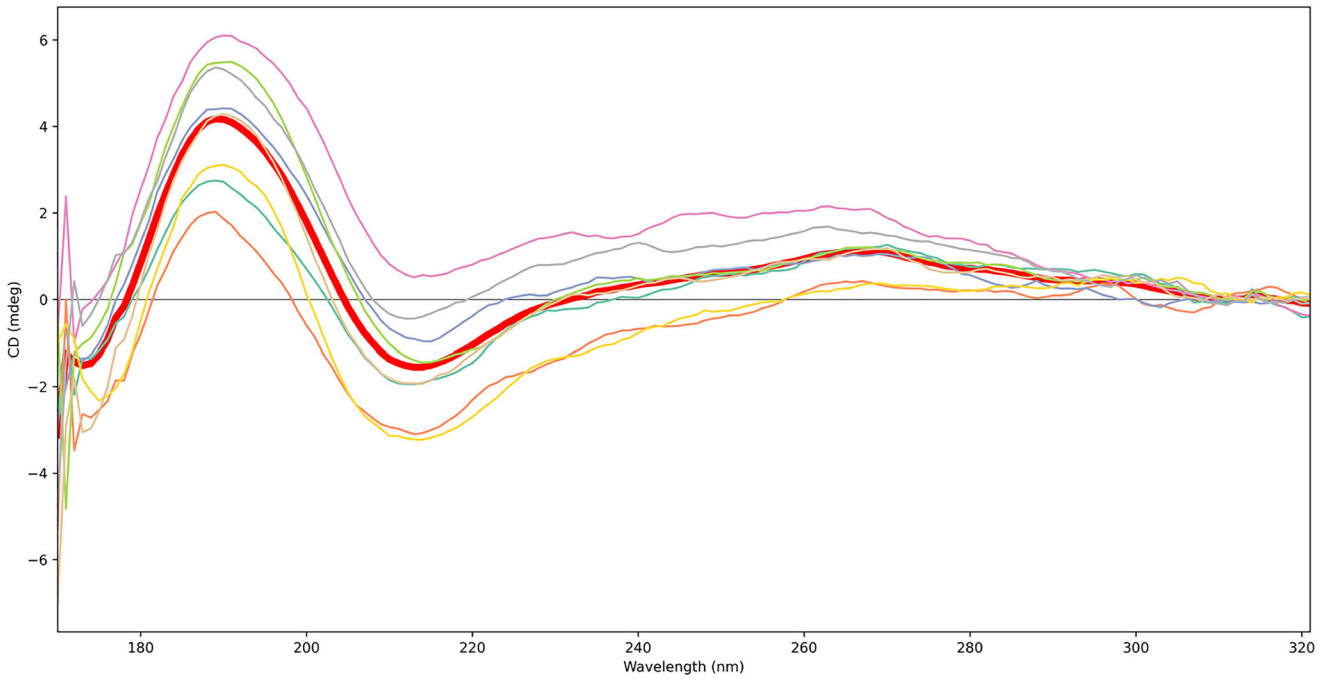

FIGURE 5 | SR-O-CD analysis of the CTR-mediated interaction of *rpsO* RNA with OMV supported membrane. Thin line: Spectra at different rotation angles obtained after washing to remove excess RNA. Red bold line: Mean of the spectra at different orientations. In the case of *rpsO*, the absence of spectral inversion indicates that there is no significant RNA insertion into the OMVs. Nevertheless, the change in the signal intensity depending on the rotation indicates that the RNA interacts with the OMVs.

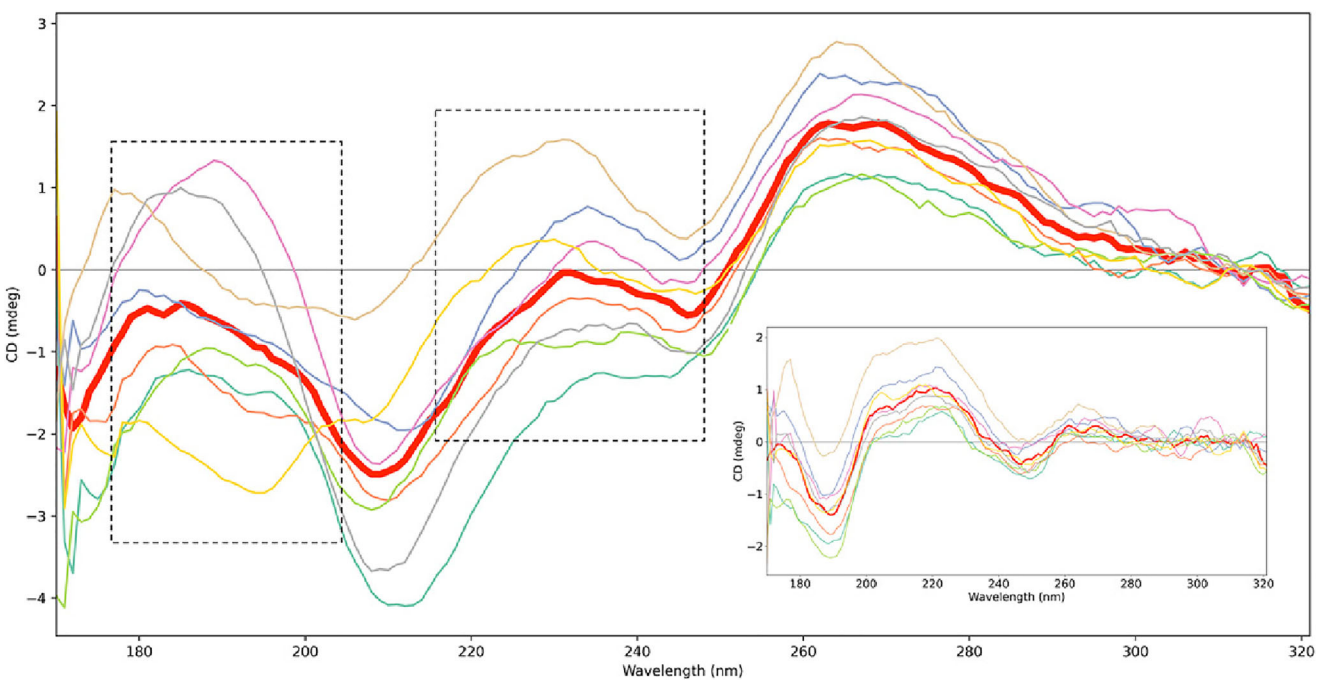

FIGURE 6 | SR-O-CD analysis of the CTR-mediated interaction of *polyA* with OMV supported membrane. Thin line: Spectra at different rotation angles obtained after washing. Red bold line: Averaged spectra of the different orientation spectra. Inset: control of CTR interaction with *polyA* and the OMV. The spectral change depending on the orientation (highlighted by black-dotted frames) indicates that a slight insertion of rA_{18} occurs in the presence of the CTR. Without CTR, the polyA does not insert in the membrane as shown in the inset of figure.

prompt further consideration of this aspect. The presence of RNAs in OMVs from various Gram-negative bacteria has been reported previously (Ahmadi Badi et al., 2020; Ghosal et al. 2015; Koeppen et al. 2016; Malabirade et al., 2018). However, their precise localization within OMVs remains unclear. OMVs contain two main types of cargo molecules: those embedded in the vesicle membrane and those enclosed within the vesicle lumen. Nucleic acids (DNA and RNA) were initially thought to belong exclusively to the latter category, that is, lumen-associated cargo (Jan 2017). Previous studies proposed that RNAs may be imported with the help of the Hfq chaperone, which could help protect them from degradation within the OMV lumen, where RNases are abundant (Hussein et al. 2023; Moll et al. 2003; Turbant et al. 2022). Other studies suggest that some RNAs may partially protrude from the OMV surface, indicating that they could be surface-bound or partially embedded within the vesicle membrane. Supporting this possibility, treatment with RNase A, which cannot cross intact membranes, selectively degraded external RNAs while leaving protected internal RNAs intact, thereby confirming the presence of RNAs associated with the OMV surface (Blache and Achouak 2024; Koeppen et al. 2016). Together, these observations suggest that OMV-associated RNAs may occupy multiple spatial localizations, including both lumenal and surface-associated positions, raising important questions about their organization and accessibility.

In this study, we also demonstrate that RNAs can be inserted into the OMV membrane (and not only lie on the surface of the vesicle). This suggests that these RNAs can be translocated from the lumen into the OMV membrane, resulting in a dual localization as both lumen- and membrane-associated cargo. We further show that this insertion process is dependent on Hfq, specifically on its amyloid-like C-terminal region, which mediates RNA translocation. Notably, the kinetics of RNA insertion observed in our experiments are relatively slow, occurring over several hours. However, under *in vivo* conditions—such as the presence of the NTR torus in full-length Hfq and the effects of macromolecular crowding—this process may be significantly accelerated or modulated. Reproducing these physiological conditions *in vitro* using the SR-O-CD setup remains challenging, underscoring the need for further investigation. The development of alternative approaches, such as single-molecule fluorescence resonance energy transfer (smFRET) could provide valuable insights into the underlying mechanism (Hwang et al. 2011). Although the Hfq-CTR mediates amyloid-like assembly in *E. coli*, its functional role in other Gram-negative bacteria remains largely unexplored. While Hfq is conserved across species, the length and sequence composition of the CTR vary considerably, and direct evidence for Hfq amyloid structures outside *E. coli* is currently limited to only a few cases (Arluison et al. 2004; Sun et al. 2002). It is therefore plausible that similar assemblies occur in other species, yet their functional relevance remains to be established. Alternatively, other proteins and/or mechanisms not involving amyloids may contribute to RNA export onto the OMV surface.

It is worth noting that our work proposes an innovative method for analysing RNA insertion into biological membranes using SR-O-CD . Several methods are available to study RNA-membrane interactions. These include techniques like fluorescence microscopy, including FRET and surface plasmon resonance (SPR) to track binding events; dynamic light scattering (DLS) or fluorescence correlation spectroscopy (FCS) to measure RNA-associated size changes; and isothermal titration calorimetry (ITC), which offers insights into RNA-lipid interactions thermodynamics. Nevertheless, these techniques do not allow discrimination between simple interaction and true insertion of RNA into the membrane. High-resolution structural techniques such as cryo-electron microscopy (Cryo-EM) and small-angle X-ray/neutron scattering (SAXS/SANS) offer detailed visualization of RNA insertion into membranes, but they are time- and/or material-consuming. In contrast, our SR-O-CD protocol offers a new, rapid, and reliable alternative to address this important question.

Our work also provides new insights into the potential mechanism by which OMV-associated RNAs may be taken up by host cells or other bacteria. Although RNA internalization into host cells has been observed, the precise mechanism remains unknown (Bittel et al. 2021). It has been proposed that RNAs could be released into the eukaryotic cytoplasm following OMV uptake by endocytosis. While recent studies have identified certain molecules as critical for OMV entry into host cells, such as LPS and the O-antigen (O'Donoghue et al. 2017), little is known about the specific factors involved in this process. Here we propose an alternative pathway, whereby OMV-associated RNAs follow distinct delivery routes to host cells. Furthermore, our results suggest that Hfq may act as a key facilitator of RNA translocation and delivery. The identification of specific OMV-associated RNAs bound to Hfq points to a potentially selective mechanism that warrants further investigation, particularly under varying stress conditions that could alter the vesicular RNA profile (Orench-Rivera and Kuehn 2021).

In summary, our research highlights the complex role of RNA in bacterial OMV function. We suggest that OMV-associated RNA may not only be delivered into eukaryotic cells by endocytosis, but can also interact with host cell membranes. This dual capability underscores the flexibility of RNA-mediated regulation and suggests that OMV-delivered RNAs may trigger various host responses, including immune activation. Furthermore, our findings expand the current understanding of bacterial OMVs as RNA-delivery platforms, highlighting new perspectives for their application in vaccine development and RNA-based therapeutics (Diallo et al., 2022a; Gao et al. 2023; Lieberman 2022; Rocha Minarini, 2024; Stanton 2021).

Author Contributions

Kevin Mosca: formal analysis, writing – original draft, methodology, software, visualization, investigation. **Florian Turbant**: methodology, investigation, formal analysis, software, visualization. **Wafa Achouak**: writing – review and editing, validation, funding acquisition, resources, conceptualization. **Frank Wien**: formal analysis, writing – original draft, writing – review and editing, software, funding acquisition, methodology, resources. **Véronique Arluison**: conceptualization, formal analysis, writing – original draft, methodology, project administration, writing – review and editing, validation, funding acquisition, resources, data curation, supervision.

Acknowledgements

We are grateful to Marisela Velez (CSIC, Madrid) for her help in TEM imaging in the framework of IEA/PICS program, to Anaïs Blache (CEA Cadarache) for her contribution during the early stages of this project, to Joana Weiler (Lübeck University, Germany), Virginie Courtois, Jean-Francois Cotte and Jean-Sebastien Bolduc (Sanofi, France), Florent Busi (Université paris Cité) and Grzegorz Wegrzyn (U. Gdansk, Poland) for critical reading of the manuscript. SRCD and SR-O-CD measurements on DISCO at the SOLEIL Synchrotron were performed under proposal 20231277.

Funding

This work has benefited from French State support as part of high-risk research program Audace!, led by the CEA and managed by the Agence Nationale de la Recherche under the France 2030 heading, bearing the reference ANR-24-RRII-0004 (WA, VA). We acknowledge funding from International Emerging action IEA/PICS 08254 (VA, FW). KM acknowledges support from the CIFRE PhD program (ANRT, grant no. 2023/0144), involving Sanofi Vaccines (Marcy l'Etoile, France) and the Laboratoire Léon Brillouin, UMR 12 CEA/CNRS (Gif-sur-Yvette, France). This study contributes to the IdEx Université de Paris ANR-18-IDEX-0001 (VA). This work is supported by a public grant overseen by the French National research Agency (ANR) as part of the « Investissements d'Avenir » program, through the "ADI 2021" project funded by the IDEX Paris-Saclay, ANR-11-IDEX-0003-02 (FT). This research was also supported by National Science Center Poland (FT).

Conflicts of Interest

K.M. is a Sanofi employee and may hold shares and/or stock options in the company. Other authors declare no competing interests exist.

Data Availability Statement

The data that support the findings of this study are available on request from the corresponding author.

References

Ahmadi Badi, S., S. P. Bruno, A. Moshiri, S. Tarashi, S. D. Siadat, and A. Masotti. 2020. "Small RNAs in Outer Membrane Vesicles and Their Function in Host-Microbe Interactions." *Frontiers in Microbiology* 11: 1209.

Ajam-Hosseini, M., F. Akhoondi, F. Parvini, and H. Fahimi. 2023. "Gram-Negative Bacterial sRNAs Encapsulated in OMVs: An Emerging Class of Therapeutic Targets in Diseases." *Frontiers in Cellular and Infection Microbiology* 13: 1305510.

Arluison, V., M. Folichon, S. Marco, et al. 2004. "The C-Terminal Domain of Escherichia Coli Hfq Increases the Stability of the Hexamer." *European Journal of Biochemistry* 271: 1258–1265.

Berbon, M., D. Martinez, E. Morvan, et al. 2023. "Hfq C-Terminal Region Forms a Beta-Rich Amyloid-Like Motif Without Perturbing the N-Terminal Sm-Like Structure." *Communications Biology* 6: 1075.

Bittel, M., P. Reichert, I. Sarfati, et al. 2021. "Visualizing Transfer of Microbial Biomolecules by Outer Membrane Vesicles in Microbe-Host-Communication in Vivo." *Journal of Extracellular Vesicles* 10: e12159.

Blache, A., and W. Achouak. 2024. "Extraction and Purification of Outer Membrane Vesicles and Their Associated RNAs." *Methods in Molecular Biology* 2741: 11–24.

Blenkiron, C., D. Simonov, A. Muthukaruppan, et al. 2016. "Uropathogenic Escherichia Coli Releases Extracellular Vesicles That Are Associated With RNA." *PLoS ONE* 11: e0160440.

Bonnington, K. E., and M. J. Kuehn. 2017. "Breaking the Bilayer: OMV Formation During Environmental Transitions." *Microbial Cell* 4: 64–66.

Bradford, M. 1976. "A Rapid and Sensitive Method for the Quantification of Microgram Quantities of Protein Utilizing the Principle of Protein-Dye Binding." *Analytical Biochemistry* 72: 248–254.

Brennan, R. G., and T. M. Link. 2007. "Hfq Structure, Function and Ligand Binding." *Current Opinion in Microbiology* 10: 125–133.

Bürck, J., P. Wadhwani, S. Fanghanel, and A. S. Ulrich. 2016. "Oriented Circular Dichroism: A Method to Characterize Membrane-Active Peptides in Oriented Lipid Bilayers." *Accounts of Chemical Research* 49: 184–192.

Coornaert, A., A. Lu, P. Mandin, M. Springer, S. Gottesman, and M. Guillier. 2010. "MicA sRNA Links the PhoP Regulon to Cell Envelope Stress." *Molecular Microbiology* 76: 467–479.

Dauros-Singorenko, P., C. Blenkiron, A. Phillips, and S. Swift. 2018. "The Functional RNA Cargo of Bacterial Membrane Vesicles." *FEMS Microbiology Letters* 365: fny023.

De Lay, N., and S. Gottesman. 2012. "A Complex Network of Small Non-Coding RNAs Regulate Motility in Escherichia coli." *Molecular Microbiology* 86: 524–538.

De Lay, N., D. J. Schu, and S. Gottesman. 2013. "Bacterial Small RNA-Based Negative Regulation: Hfq and Its Accomplices." *Journal of Biological Chemistry* 288: 7996–8003.

Diallo, I., J. Ho, D. Lalaouna, E. Masse, and P. Provost. 2022a. "RNA Sequencing Unveils Very Small RNAs With Potential Regulatory Functions in Bacteria." *Frontiers in Molecular Biosciences* 9: 914991.

Diallo, I., J. Ho, M. Lambert, et al. 2022b. "A tRNA-Derived Fragment Present in E. Coli OMVs Regulates Host Cell Gene Expression and Proliferation." *PLOS Pathogens* 18: e1010827.

Diestra, E., B. Cayrol, V. Arluison, and C. Risco. 2009. "Cellular Electron Microscopy Imaging Reveals the Localization of the Hfq Protein Close to the Bacterial Membrane." *PLoS ONE* 4: e8301.

Eason, I. R., H. P. Kaur, K. A. Alexander, and M. V. Sukhodolets. 2019. "Growth Phase-Specific Changes in the Composition of E. Coli Transcription Complexes." *Journal of Chromatography B, Analytical Technologies in the Biomedical and Life Sciences* 1109: 155–165.

Folichon, M., V. Arluison, O. Pellegrini, E. Huntzinger, P. Regnier, and E. Hajnsdorf. 2003. "The Poly(A) Binding Protein Hfq Protects RNA From RNase E and Exoribonucleolytic Degradation." *Nucleic Acids Research* 31: 7302–7310.

Fortas, E., F. Piccirilli, A. Malabirade, et al. 2015. "New Insight Into the Structure and Function of Hfq C-Terminus." *Bioscience Reports* 35: e00190.

Frohlich, K. S., and S. Gottesman. 2018. "Small Regulatory RNAs in the Enterobacterial Response to Envelope Damage and Oxidative Stress." *Microbiology Spectrum* 6. https://doi.org/10.1128/microbiolspec.rwr-0022-2018.

Furuyama, N., and M. P. Sircili. 2021. "Outer Membrane Vesicles (OMVs) Produced by Gram-Negative Bacteria: Structure, Functions, Biogenesis, and Vaccine Application." *BioMed research international* 2021: 1490732.

Gao, X., Y. Li, G. Nie, and X. Zhao. 2023. "mRNA Delivery Platform Based on Bacterial Outer Membrane Vesicles for Tumor Vaccine." *Bio-protocol* 13: e4774.

Gelsinger, D. R., and J. DiRuggiero. 2018. "The Non-Coding Regulatory RNA Revolution in Archaea." *Genes* 9: 141.

Ghosal, A., B. B. Upadhyaya, J. V. Fritz, et al. 2015. "The Extracellular RNA Complement of Escherichia Coli." *MicrobiologyOpen* 4: 252–266.

Gonzalez, M. J., N. Navarro, E. Cruz, et al. 2024. "First Report on the Physicochemical and Proteomic Characterization of Proteus Mirabilis Outer Membrane Vesicles Under Urine-Mimicking Growth Conditions: Comparative Analysis With Escherichia Coli." *Frontiers in Microbiology* 15: 1493859.

Gottesman, S. 2019. "Trouble Is Coming: Signaling Pathways That Regulate General Stress Responses in Bacteria." *Journal of Biological Chemistry* 294: 11685–11700.

Ha, J. Y., S. Y. Choi, J. H. Lee, S. H. Hong, and H. J. Lee. 2020. "Delivery of Periodontopathogenic Extracellular Vesicles to Brain Monocytes and Microglial IL-6 Promotion by RNA Cargo." *Frontiers in Molecular Biosciences* 7: 596366.

Hajnsdorf, E., F. Braun, J. Haugel-Nielsen, and P. Regnier. 1995. "Polyadenylylation Destabilizes the rpsO mRNA of Escherichia coli." *Proceedings of the National Academy of Sciences of the United States of America* 92: 3973–3977.

Hajnsdorf, E., and P. Régnier. 2000. "Host Factor HFq of *Escherichia Coli* Stimulates Elongation of Poly(A) Tails by Poly(A)Polymerase I." *Proceedings of the National Academy of Sciences of the United States of America* 97: 1501–1505.

Haugel-Nielsen, J., E. Hajnsdorf, and P. Regnier. 1996. "The rpsO mRNA of Escherichia Coli Is Polyadenylated at Multiple Sites Resulting From Endonucleolytic Processing and Exonucleolytic Degradation." *EMBO Journal* 15: 3144–3152.

Hoffmann, S. V., N. C. Jones, and A. Rodger. 2026. "Couette Flow Linear Dichroism Spectroscopy." *Methods in Molecular Biology* 3004: 105–121.

Hussein, M., R. Jasim, H. Gocol, et al. 2023. "Comparative Proteomics of Outer Membrane Vesicles from Polymyxin-Susceptible and Extremely Drug-Resistant Klebsiella Pneumoniae." *mSphere* 8: e0053722.

Hwang, W., V. Arluison, and S. Hohng. 2011. "Dynamic Competition of DsrA and rpoS Fragments for the Proximal Binding Site of Hfq as a Means for Efficient Annealing." *Nucleic Acids Research* 39: 5131–5139.

Ikeda, Y., M. Yagi, T. Morita, and H. Aiba. 2011. "Hfq Binding at RhlB-Recognition Region of RNase E Is Crucial for the Rapid Degradation of Target mRNAs Mediated by sRNAs in Escherichia Coli." *Molecular Microbiology* 79: 419–432.

Jan, A. T. 2017. "Outer Membrane Vesicles (OMVs) of Gram-Negative Bacteria: A Perspective Update." *Frontiers in Microbiology* 8: 1053.

Kannaiah, S., J. Livny, and O. Amster-Choder. 2019. "Spatiotemporal Organization of the E. Coli Transcriptome: Translation Independence and Engagement in Regulation." *Molecular Cell* 76: 574–589.e7.

Kavita, K., F. de Mets, and S. Gottesman. 2018. "New Aspects of RNA-Based Regulation by Hfq and Its Partner sRNAs." *Current Opinion in Microbiology* 42: 53–61.

Koeppen, K., T. H. Hampton, M. Jarek, et al. 2016. "A Novel Mechanism of Host-Pathogen Interaction Through sRNA in Bacterial Outer Membrane Vesicles." *PLOS Pathogens* 12: e1005672.

Kulp, A., and M. J. Kuehn. 2010. "Biological Functions and Biogenesis of Secreted Bacterial Outer Membrane Vesicles." *Annual Review of Microbiology* 64: 163–184.

Kuscu, C., P. Kumar, M. Kiran, Z. Su, A. Malik, and A. Dutta. 2018. "tRNA Fragments (tRFs) Guide Ago to Regulate Gene Expression Post-Transcriptionally in a Dicer-Independent Manner." *RNA* 24: 1093–1105.

Lee, H. J. 2019. "Microbe-Host Communication by Small RNAs in Extracellular Vesicles: Vehicles for Transkingdom RNA Transportation." *International Journal of Molecular Sciences* 20: 1487.

Lieberman, L. A. 2022. "Outer Membrane Vesicles: A Bacterial-Derived Vaccination System." *Frontiers in Microbiology* 13: 1029146.

Liu, H., X. Wang, H. D. Wang, et al. 2012. "Escherichia Coli Noncoding RNAs Can Affect Gene Expression and Physiology of Caenorhabditis elegans." *Nature Communications* 3: 1073.

Maes, A., C. Gracia, N. Innocenti, K. Zhang, E. Aurell, and E. Hajnsdorf. 2017. "Landscape of RNA Polyadenylation in E. Coli." *Nucleic Acids Research* 45: 2746–2756.

Majdalani, N., C. Cunning, D. Sledjeski, T. Elliott, and S. Gottesman. 1998. "DsrA RNA Regulates Translation of RpoS Message by an Anti-Antisense Mechanism, Independent of Its Action as an Antisilencer of Transcription." *PNAS* 95: 12462–12467.

Malabirade, A., J. Habier, A. Heintz-Buschart, et al. 2018. "The RNA Complement of Outer Membrane Vesicles from *Salmonella Enterica* Serovar Typhimurium under Distinct Culture Conditions." *Frontiers in Microbiology* 9: 2015.

Malabirade, A., J. Morgado-Brajones, S. Trepout, et al. 2017. "Membrane Association of the Bacterial Riboregulator Hfq and Functional Perspectives." *Scientific Reports* 7: 10724.

Mancini, F., O. Rossi, F. Necchi, and F. Micoli. 2020. "OMV Vaccines and the Role of TLR Agonists in Immune Response." *International Journal of Molecular Sciences* 21: 4416.

Melamed, S., P. P. Adams, A. Zhang, H. Zhang, and G. Storz. 2020. "RNA-RNA Interactomes of ProQ and Hfq Reveal Overlapping and Competing Roles." *Molecular Cell* 77: 411–425.e417.

Miles, A. J., and B. A. Wallace. 2006. "Synchrotron Radiation Circular Dichroism Spectroscopy of Proteins and Applications in Structural and Functional Genomics." *Chemical Society Reviews* 35: 39–51.

Miles, A. J., and B. A. Wallace. 2018. "CDtoolX, a Downloadable Software Package for Processing and Analyses of Circular Dichroism Spectroscopic Data." *Protein Science* 27: 1717–1722.

Moll, I., T. Afonyushkin, O. Vytvytska, V. R. Kaberdin, and U. Blasi. 2003. "Coincident Hfq Binding and RNase E Cleavage Sites on mRNA and Small Regulatory RNAs." *Rna* 9: 1308–1314.

Mosca, K., V. Arluison, and F. Wien. 2026. "Application of Synchrotron Radiation Circular Dichroism for Structural Analysis of RNAs." *Methods in Molecular Biology* 3004: 41–57.

O'Donoghue, E. J., N. Sirisaengtaksin, D. F. Browning, et al. 2017. "Lipopolysaccharide Structure Impacts the Entry Kinetics of Bacterial Outer Membrane Vesicles Into Host Cells." *Plos Pathogens* 13: e1006760.

Obregon, K. A., C. T. Hoch, and M. V. Sukhodolets. 2015. "Sm-Like Protein Hfq: Composition of the Native Complex, Modifications, and Interactions." *Biochimica et Biophysica Acta* 1854: 950–966.

Olsen, A. S., J. Moller-Jensen, R. G. Brennan, and P. Valentin-Hansen. 2010. "C-Terminally Truncated Derivatives of Escherichia coli Hfq Are Proficient in Riboregulation." *Journal of Molecular Biology* 404: 173–182.

Orench-Rivera, N., and M. J. Kuehn. 2021. "Differential Packaging into Outer Membrane Vesicles Upon Oxidative Stress Reveals a General Mechanism for Cargo Selectivity." *Frontiers in Microbiology* 12: 561863.

Pandey, S., T. Kawai, and S. Akira. 2014. "Microbial Sensing by Toll-Like Receptors and Intracellular Nucleic Acid Sensors." *Cold Spring Harbor Perspectives in Biology* 7: a016246.

Papenfort, K., and S. Melamed. 2023. "Small RNAs, Large Networks: Posttranscriptional Regulons in Gram-Negative Bacteria." *Annual Review of Microbiology* 77: 23–43.

Pulvermacher, S. C., L. T. Stauffer, and G. V. Stauffer. 2009. "Role of the Escherichia coli Hfq Protein in GcvB Regulation of oppA and dppA mRNAs." *Microbiology* 155: 115–123.

Qiang, W., W. M. Yau, and J. Schulte. 2015. "Fibrillation of Beta Amyloid Peptides in the Presence of Phospholipid Bilayers and the Consequent Membrane Disruption." *Biochimica Et Biophysica Acta* 1848: 266–276.

Rice, J. B., and C. K. Vanderpool. 2011. "The Small RNA SgrS Controls Sugar-phosphate Accumulation by Regulating Multiple PTS Genes." *Nucleic Acids Research* 39: 3806–3819.

Rocha Minarini, L. A. D. 2024. "Exploring Bacterial Extracellular Vesicles: Focus on WHO Critical Priority Pathogens." *Current Topics in Membranes* 94: 225–246.

Salim, N. N., M. A. Faner, J. A. Philip, and A. L. Feig. 2012. "Requirement of Upstream Hfq-binding (ARN)X Elements in glmS and the Hfq C-Terminal Region for GlmS Upregulation by sRNAs GlmZ and GlmY." *Nucleic Acids Research* 40: 8021–8032.

Salvail, H., and E. Masse. 2012. "Regulating Iron Storage and Metabolism With RNA: An Overview of Posttranscriptional Controls of Intracellular Iron Homeostasis." *Wiley Interdisciplinary Reviews: RNA* 3: 26–36.

Sartorio, M. G., E. J. Pardue, M. F. Feldman, and M. F. Haurat. 2021. "Bacterial Outer Membrane Vesicles: From Discovery to Applications." *Annual Review of Microbiology* 75: 609–630.

Schwechheimer, C., and M. J. Kuehn. 2015. "Outer-Membrane Vesicles From Gram-Negative Bacteria: Biogenesis and Functions." *Nature Reviews Microbiology* 13: 605–619.

Shih, P., D. R. Holland, and J. F. Kirsch. 1995. "Thermal Stability Determinants of Chicken Egg-White Lysozyme Core Mutants: Hydrophobicity, Packing Volume, and Conserved Buried Water Molecules." *Protein Science* 4: 2050–2062.

Shimizu, T. 2024. "RNA Recognition in Toll-Like Receptor Signaling." *Current Opinion in Structural Biology* 88: 102913.

Stanton, B. A. 2021. "Extracellular Vesicles and Host-Pathogen Interactions: A Review of Inter-Kingdom Signaling by Small Noncoding RNA." *Genes* 12: 1010.

Sun, X., I. Zhulin, and R. M. Wartell. 2002. "Predicted Structure and Phyletic Distribution of the RNA-Binding Protein Hfq." *Nucleic Acids Research* 30: 3662–3671.

Svensson, S. L., and C. M. Sharma. 2016. "Small RNAs in Bacterial Virulence and Communication." *Microbiology Spectrum* 4. https://doi.org/10.1128/microbiolspec.VMBF-0028-2015.

Taghbalout, A., Q. Yang, and V. Arluison. 2014. "The Escherichia coli RNA Processing and Degradation Machinery Is Compartmentalized Within an Organized Cellular Network." *Biochemical Journal* 458: 11–22.

Tsatsaronis, J. A., S. Franch-Arroyo, U. Resch, and E. Charpentier. 2018. "Extracellular Vesicle RNA: A Universal Mediator of Microbial Communication?" *Trends in Microbiology* 26: 401–410.

Turbant, F., A. Blache, G. Wegrzyn, W. Achouak, F. Wien, and V. Arluison. 2024a. "Use of Synchrotron Radiation Circular Dichroism to Analyze the Interaction and Insertion of Proteins Into Bacterial Outer Membrane Vesicles." *Methods in Molecular Biology* 2843: 73–94.

Turbant, F., Q. Machiels, J. Waeytens, F. Wien, and V. Arluison. 2024b. "The Amyloid Assembly of the Bacterial Hfq Is Lipid-Driven and Lipid-Specific." *International Journal of Molecular Sciences* 25: 1434.

Turbant, F., J. Waeytens, A. Blache, et al. 2023. "Interactions and Insertion of Escherichia Coli Hfq Into Outer Membrane Vesicles as Revealed by Infrared and Orientated Circular Dichroism Spectroscopies." *International Journal of Molecular Sciences* 24: 11424.

Turbant, F., J. Waeytens, C. Campidelli, et al. 2022. "Unraveling Membrane Perturbations Caused by the Bacterial Riboregulator Hfq." *International Journal of Molecular Sciences* 23: 8739.

Turbant, F., P. Wu, F. Wien, and V. Arluison. 2021. "The Amyloid Region of Hfq Riboregulator Promotes DsrA:rpoS RNAs Annealing." *Biology* 10: 900.

Vecerek, B., L. Rajkowitsch, E. Sonnleitner, R. Schroeder, and U. Blasi. 2008. "The C-Terminal Domain of Escherichia coli Hfq Is Required for Regulation." *Nucleic Acids Research* 36: 133–143.

Vigoda, M. B., L. Argaman, M. Kournos, and H. Margalit. 2024. "Unraveling the Interplay Between a Small RNA and RNase E in Bacteria." *Nucleic Acids Research* 52: 8947–8966.

Vincent, H. A., C. A. Henderson, C. M. Stone, et al. 2012. "The Low-Resolution Solution Structure of Vibrio Cholerae Hfq in Complex With Qrr1 sRNA." *Nucleic Acids Research* 40: 8698–8710.

Vogel, J., and B. F. Luisi. 2011. "Hfq and Its Constellation of RNA." *Nature Reviews Microbiology* 9: 578–589.

Waeytens, J., F. Turbant, V. Arluison, V. Raussens, and F. Wien. 2022. "Analysis of Bacterial Amyloid Interaction With Lipidic Membrane by Orientated Circular Dichroism and Infrared Spectroscopies." *Methods in Molecular Biology* 2538: 217–234.

Welsh, J. A., D. C. I. Goberdhan, L. O'Driscoll, et al. 2024. "Minimal Information for Studies of Extracellular Vesicles (MISEV2023): From Basic to Advanced Approaches." *Journal of Extracellular Vesicles* 13: e12404.

Wien, F., M. Paternostre, F. Gobeaux, F. Artzner, and M. Refregiers. 2013. "Calibration and Quality Assurance Procedures at the Far UV Linear and Circular Dichroism Experimental Station DISCO." *Journal of Physics: Conference Series (JPCS)* 425: 122014.

Wien, F., and B. A. Wallace. 2005. "Calcium Fluoride Micro Cells for Synchrotron Radiation Circular Dichroism Spectroscopy." *Applied Spectroscopy* 59: 1109–1113.

Wu, Y., H. W. Huang, and G. A. Olah. 1990. "Method of Oriented Circular Dichroism." *Biophysical Journal* 57: 797–806.

Zhang, X., W. Ding, J. Yang, et al. 2025. "Mechanisms of Outer Membrane Vesicles in Bacterial Drug Resistance: Insights and Implications." *Biochimie* 238: 77–90.

Supporting Information

Additional supporting information can be found online in the Supporting Information section.

Supporting Information: **Figure S1**. UV absorbance spectrum of OMVs. The UV absorbance spectrum recorded during CD measurements shows a detectable signal at 260 nm, indicating the presence of nucleic acids at low levels. From an absorbance of 0.018 at 260 nm, the RNA concentration is estimated at ∼52 μg/mL (≈150 μM in nucleotide units), corresponding to ∼0.6 nmol of RNA in the SR-O-CD sample. The 260/280 ratio of 1.88 suggests that the signal mainly originates from nucleic acids, most likely RNA, although a minor protein contribution cannot be excluded. **Figure S2**. Transmission Electron Microscopy (TEM) analysis after negative staining using 0.1% phosphotungstic acid. (A) Before density gradient purification. The image confirms the absence of significant amounts of flagella, fimbriae, and pili in the OMV preparations from the Δhfq strain. Additionally, no evidence of a substantial population of outer–inner membrane vesicles (OIMVs) was observed, even prior to gradient purification. (B) TEM analysis after density gradient purification. OMVs isolated from the Δhfq strain ranged in diameter from 20 to 100 nm on average.